Annals of Biomedical Engineering, Vol. 35, No. 9, September 2007 *(© 2007)* pp. 1595–1607
DOI: 10.1007/s10439-007-9324-8

A Quantitative Model of Gastric Smooth Muscle Cellular Activation

ALBERTO CORRIAS and MARTIN L. BUIST

Division of Bioengineering, National University of Singapore, 9 Engineering Drive 1, Singapore 117576, Singapore

(Received 5 September 2006; accepted 24 April 2007; published online 8 May 2007)

Abstract—A physiologically realistic quantitative description of the electrical behavior of a gastric smooth muscle (SM) cell is presented. The model describes the response of a SM cell when activated by an electrical stimulus coming from the network of interstitial cells of Cajal (ICC) and is mediated by the activation of different ion channels species in the plasma membrane. The conductances (predominantly Ca^{2+} and K^{+}) that are believed to substantially contribute to the membrane potential fluctuations during slow wave activity have been included in the model. A phenomenological description of intracellular Ca^{2+} dynamics has also been included because of its primary importance in regulating a number of cellular processes. In terms of shape, duration, and amplitude, the resulting simulated smooth muscle depolarizations (SMDs) are in good agreement with experimentally recordings from mammalian gastric SM in control and altered conditions. This model has also been designed to be suitable for incorporation into large scale multicellular simulations.

Keywords—Gastric muscle, Electrophysiology, Computational model.

INTRODUCTION

Gastric motility is achieved through the coordinated activity of the enteric nervous system (ENS), interstitial cells of Cajal (ICC), and smooth muscle (SM) cells. ICC are responsible for the omnipresent electrical activity intrinsic to the stomach musculature, whereas the ENS constitutes an additional, extrinsic, level of control. ICC and the ENS supply SM cells with the necessary stimuli to contract and their coordinated contraction generates motility. Although ICC variants have been found in several locations within the stomach wall, the ICC of the myenteric plexus (ICC-MY), which lies between the circular and longitudinal SM layers, are considered largely responsible for the generation and maintenance of slow wave activity. Another ICC variant, the intramuscular ICC (ICC-IM), also appears to have pacemaking capabilities and is believed to play a role in propagating slow wave activity through the relatively thick SM layers. These regular autonomous depolarizations are then propagated via gap junctions to the neighboring circular and longitudinal SM cells.

At present, it appears somewhat unclear as to what terminology should be used to describe this SM electrical activity. In their review, Sanders *et al.*[43] summarized the terminology that is currently in use. In SM cells the terms 'slow wave' and 'follower potential' have been used to describe such electrical events. Unfortunately the former is more commonly associated with ICC activity whereas the latter has been used only in the context of longitudinal SM cells. In order to avoid any ambiguity, in the present work the term *smooth muscle depolarization* (SMD) will be used to describe the cellular response of a SM cell when stimulated electrically by an ICC and the term slow wave will be used to describe activity within the ICC network.

SM cells, the focus of this study, do not appear to possess the ability to generate or actively propagate slow waves. Their response to an electrical stimulus provided by the neighboring ICC network is mediated by the activation of a wide variety of voltage-dependent ion channels within their cell membrane. The response of a SM cell is further regulated by extracellular ligands and intracellular second messengers (Ca^{2+} being one of the most prominent). In such a complex system it is difficult to quantify the contribution of each component to the overall response of the cell. Mathematical models can succinctly describe the results from a large number of experiments and thus provide an invaluable tool to aid in developing our understanding of the physiology and pathophysiology of gastric electrical activity. Such an approach is not without precedent. Over the past few decades computational models of cardiac electrophysiology have advanced significantly, from the single cell level to whole tissue simulations (reviewed in Noble[38]). This approach has been very successful to the point where genetic disorders that result in ion channelopathies

Address correspondence to Martin L. Buist, Division of Bioengineering, National University of Singapore, 9 Engineering Drive 1, Singapore 117576, Singapore. Electronic mail: biebml@nus.edu.sg

have now been directly linked to cardiac conditions and consequent abnormalities in the electrocardiogram (e.g., Splawski *et al.*[48]).

At present, integrated modeling of the gastric electrophysiology is inhibited by a lack of the single cell models that form the building blocks on which more complex models rely. Existing electrophysiological descriptions of the gastric musculature[12,40] rely upon equations that attempt to describe the behavior of a single cell but are not based on the underlying biological processes that cause the observed fluctuations in cell membrane potential. Moreover, our knowledge of the different nature and functionality of SM cells and ICC is relatively recent and consequently a number of previously published works do not incorporate this distinction (e.g., Mifthakov *et al.*[33]). Similarly, Skinner *et al.*[46] developed a generic model of SM electrophysiology that is now inconsistent with current experimental data. An attempt to describe the underlying electrophysiology of a generic SM was made by Lang and Rattray-Wood.[31] Their relatively simple mathematical model takes into account some of the major ionic currents but is not aimed to describe a specific type of SM. More recently, Aliev *et al.*[2] developed a mathematical description of the electrical activity of the intestine by tuning the parameters of the widely used Fitzhugh–Nagumo model to obtain a description of both slow wave and SMD activity but again, these parameters have no biological correlate. We present here a mathematical description of single cell gastric SM electrophysiology, constructed from the predominant aspects of the underlying physiology and fitted to published experimental data. The model has also been designed to be computationally efficient and is therefore suitable for inclusion in multi-cellular simulations.

MATERIALS AND METHODS

Following the classical Hodgkin–Huxley approach, the cell membrane was described by an equivalent circuit consisting of a capacitance connected in parallel with variable conductances representing the different pathways for ion movement.

$$\frac{dV_m}{dt} = -\frac{1}{C_m}(I_{ion} + I_{stim}) \tag{1}$$

Here V_m (in mV) is the membrane potential, C_m (in pF) is the cell capacitance, I_{stim} (in pA) is a stimulus current supplied by the ICC network, and I_{ion} (in pA) represents the sum of the ionic currents crossing the cell membrane, the details of which are given below. The gating mechanisms and kinetics were modelled with Hodgkin & Huxley-type variables (see Eq. 2) unless otherwise specified where g is the gating variable, g_∞ is its steady state value and τ_g is the time constant.

$$\frac{dg}{dt} = \frac{g_\infty - g}{\tau_g} \tag{2}$$

Figure 1 shows a schematic view of the main ion channels and intracellular components that were included in the model.

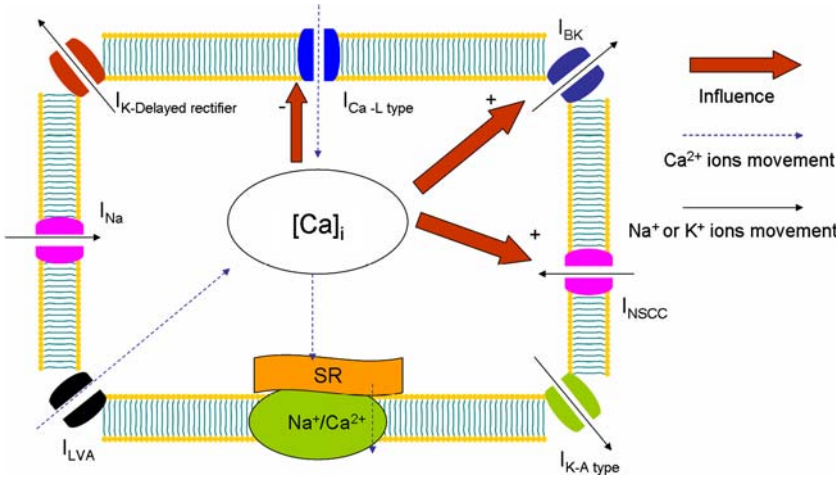

FIGURE 1. A schematic view of the main components that have been included in the model. L-type and low voltage activated Ca^{2+} channels, delayed rectifier, A-type and Ca^{2+}-activated potassium channels, sodium channels and non-selective cationic channels are included in the plasma membrane. For each channel the arrow indicates the direction of ionic flux (dashed arrow for Ca^{2+} ions, solid arrow for sodium or potassium ions). A phenomenological description of the sarcoplasmic reticulum (SR) and Na^+/Ca^{2+} exchanger have also been included to regulate the intracellular Ca^{2+} transient. The role of Ca^{2+} as second messenger is represented with bold arrows accompanied by a '+' when the effect is an enhanced action and '–' when the effect is an inhibitory action.

L-type Calcium Current

I_{CaL} represents the influx of Ca^{2+} ions through voltage-gated, Dihydropyridine (DHP)-sensitive L-type Ca^{2+} channels that are commonly expressed in the muscle cells of mammalian organisms.

$$I_{CaL} = G_{CaL} * d * f * f_{Ca} * (V_m - E_{Ca}) \quad (3)$$

Here E_{Ca} is the Nernst potential for Ca^{2+}, calculated using concentration data.[10,28] G_{CaL} is the maximum channel conductance whose value (65 nS) was chosen to reproduce the Ca^{2+} current characteristics recorded in voltage clamp experiments on canine gastric SM cells.[56] d and f are Hodgkin–Huxley type activation and inactivation gating variables respectively. Measurements of the steady state voltage dependency of d and f in SM cells from guinea pig taenia coli,[63] canine jejunum,[14] human colon[61] and canine colon[32] have shown prominent inter-organ variability. The half maximal values for the steady state activation vary from 6 mV in the canine jejunum[14] to 27.5 mV in the human colon.[61] In the absence of direct experimental data from the stomach for the steady state activation gating variable, we have adopted the formulation of Akbarali *et al.*[1] where the half maximal value for the steady state activation was 17 mV. The steady state inactivation curve was taken from experiments on canine gastric SM.[56] Inactivation kinetics have been measured in human[61] and canine[29] colonic myocytes as well as canine pyloric myocytes.[54] The time constant was taken from the pyloric myocyte study (86 ms) which also showed the process to be largely voltage independent. Both activation and inactivation rate constants were measured during experiments at room temperature and have been adjusted to 37 °C using a Q_{10} of 2.1.[13]

Ca^{2+} dependent inactivation of the L-type Ca^{2+} current has been observed experimentally where an accumulation of intracellular Ca^{2+} reduces the Ca^{2+} conductance and provides a negative feedback mechanism to control Ca^{2+} influx.[16,56] This has been incorporated into the model through a Ca^{2+} dependent inactivation variable, f_{Ca}. The steady state equation for the f_{Ca}variable was estimated using data from canine gastric SM experiments.[56] By comparing the difference in the peak current elicited when Ba^{2+} or Ca^{2+} were used as the charge carrier at different voltages in conjunction with the corresponding changes in intracellular Ca^{2+} concentration, six data points were manually extrapolated and the following equation was fitted ($R^2 = 0.94$) to these points to obtain the steady state behavior.

$$f_{Ca\infty} = 1 - \frac{1}{1 + e^{-\frac{\Delta[Ca]_i - h_{Ca}}{s_{Ca}}}} \quad (4)$$

Here $\Delta[Ca]_i$ is the variation of cytoplasmic concentration (in nM) from the value in resting conditions, while h_{Ca} and s_{Ca} are the half concentration and slope factor, respectively. In absence of data from gastric smooth muscle, we have adopted the formulation of ten Tusscher *et al.*[50] for the rate constant of f_{Ca}.

Low Voltage Activated Calcium Current

I_{LVA} represents the low voltage-activated, fast-inactivating, DHP-insensitive component of the inward current that has been described in several types of SM cells[13,53,63–65] and is often termed a 'T-type' Ca^{2+} current.

$$I_{LVA} = G_{LVA} * d_{LVA} * f_{LVA} * (V_m - E_{Ca}) \quad (5)$$

G_{LVA} is the maximum conductance of the channel and its value (0.18 nS) was chosen to reproduce voltage clamp experiments in canine gastric SM cells (in combination with I_{CaL}).[55] The resulting reproduction is illustrated in Fig. 2. d_{LVA} and f_{LVA} are Hodgkin–Huxley type activation and inactivation gating variables respectively and their steady-state kinetics were chosen to match experimental observations from *Bufo Marinus* gastric SM cells.[53] Since this current was found to have an activation threshold at −50 mV and was still active at −10 mV, half maximal values of −27.5 mV and −18.8 mV were chosen for steady state activation and inactivation respectively. The activation time constant was obtained from time-to-peak data obtained by Vivaudou *et al.*, 1988 and had a value of 3 ms. The weak voltage dependency of the inactivation time constant was described by fitting to experimental data from *Bufo Marinus* stomach[53] at −30 mV and −40mV and from guinea pig taenia coli[63] at more depolarized voltages.

Delayed Rectifier Potassium Channels

I_{Kr} refers to the typically TEA and 4-AP sensitive delayed rectifier potassium channels commonly expressed in a wide variety of excitable cells. The Nernst potential, E_K, was calculated using concentration data.[10,28]

$$I_{Kr} = G_{Kr} * x_{r1} * x_{r2} * (V_m - E_k) \quad (6)$$

Here G_{Kr} is the maximum conductance and its value (35 nS) was obtained from the slope of the predominantly linear I–V plot resulting from patch-clamp experiments in canine gastric smooth muscle.[44] In the absence of quantitative gastric data, the steady-state and time constant formulations for the Hodgkin–Huxley type activation (x_{r1}) and inactivation (x_{r2}) gating variables were taken from the

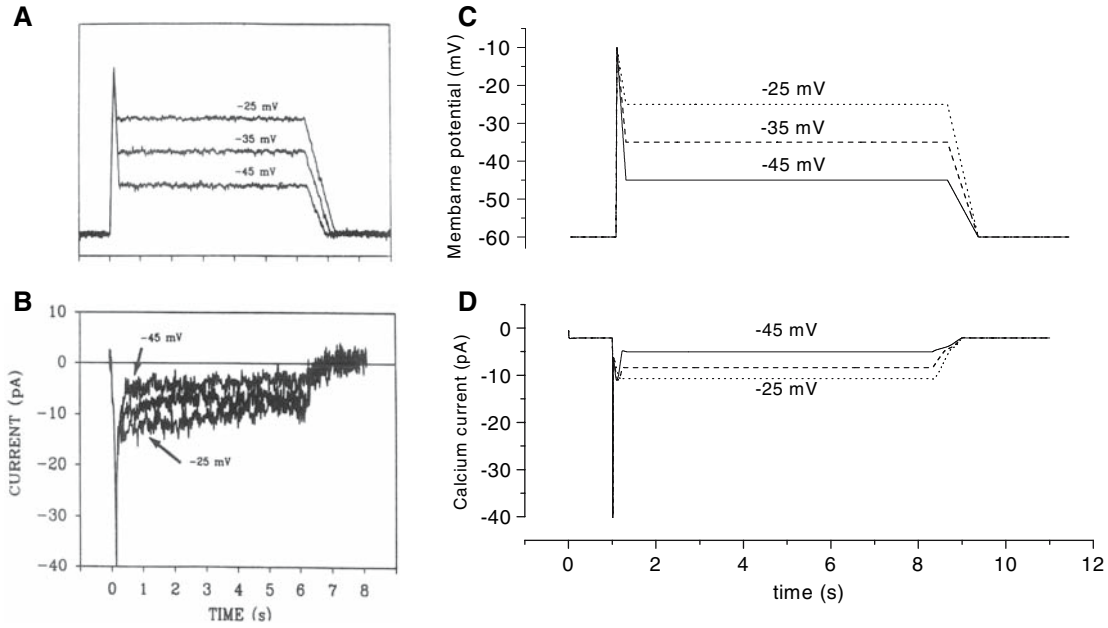

FIGURE 2. Experimental basis for the model description of Ca^{2+} currents: (a) Voltage clamp protocol applied to canine gastric SM; (b) Ca^{2+} currents elicited by the voltage clamp protocols in (a) in canine gastric smooth muscle cells; (c) Simulated voltage clamp protocol; (d) Simulation of Ca^{2+} currents ($I_{CaL} + I_{LVA}$) elicited by the voltage clamp protocol shown in (c). (a) and (b) are reproduced from Vogalis *et al.*[55] with permission.

colonic myocyte data of Koh *et al.*[30] where two time constants were required to properly represent the potassium inactivation kinetics. Both activation and inactivation time constants were corrected for the temperature difference between experiments (21 °C) and physiological conditions (37 °C) by using a Q_{10} value of 1.5.[52]

A-Type Potassium Channels

I_{KA} refers to the fast inactivating, Ca^{2+}-independent, TEA-insensitive, outward K^+ current that was first described in mollusc neurons.[4,13,17]

$$I_{KA} = G_{KA} * x_{A1} * x_{A2} * (V_m - E_k) \quad (7)$$

The maximal conductance G_{KA} was fitted in the same manner as G_{Kr}. Here a value of 9 nS was obtained from experiments on guinea pig gastric myocytes.[37] The steady state equations for the activation (x_{A1}) and inactivation (x_{A2}) Hodgkin–Huxley type gating variables have been taken from data from murine gastric smooth muscle.[3] Similar values were also found in cells from newborn rat ileum[47] and are consistent with the notion that A-type channels are almost completely inactivated at −50mV. The activation time constants were fitted from the time-to-peak data from Amberg *et al.*[3] The value of the inactivation time constant was chosen to be 90 ms in agreement with experimental data from murine gastric SM cells.[3]

Large Conductance Calcium-Activated Potassium Channels

Ca^{2+}-activated K^+ channels have been traditionally divided in three categories according to their large (BK), intermediate (IK) or small (SK) conductance. IK and SK have been implicated as mediators of inhibitory signals from the ENS for the generation of inhibitory junction potentials.[13] In our description of gastric SMDs, we therefore included only BK channels through the current I_{BK}.

$$I_{BK} = G_{BK} * P_0 * (V_m - E_k) \quad (8)$$

G_{BK} represents the temperature dependent maximal conductance.[5] BK channels appeared not to inactivate therefore an inactivation gating variable has not been included. P_0 represents the Ca^{2+}-dependent open probability which has been quantitatively described for the gastrointestinal tract.[9]

$$P_0 = \frac{1}{1 + e^{\frac{V_m}{K_{BK}} - h_{BK} * \log\frac{[Ca]_i}{Ca_{set}}}} \quad (9)$$

K_{BK}, Ca_{set} and h_{BK} values were taken from the formulation proposed in the original paper for data from canine colonic myocytes.

Sodium Channels

The presence, genotype and function of sodium channels in the gastrointestinal tract have been the

subject of some debate. The variety of IC_{50} values for the best known sodium channel blocker, TTX, underlies a probable variety of isoforms expressed throughout the gastrointestinal tract.[42] Sodium currents have been reported in guinea-pig gastric fundus[36] and, more recently, in human jejunal SM.[19] It has also been shown that TTX (up to 1 μM) does not affect the shape, amplitude, and propagation of slow waves and SMD in the guinea-pig gastric antrum.[20] We have therefore chosen to include the relatively TTX-resistant sodium channel that was described by Holm *et al.*[19] This channel was unaffected by presence of 100 nM of TTX and its amplitude was reduced by only 30% in the presence of 1 μM TTX.

$$I_{Na} = G_{Na} * d_{Na} * f_{Na} * (V_m - E_{Na}) \quad (10)$$

G_{Na} represents the maximal Na^+ conductance and its value (3 nS) was chosen to reproduce the experimental observation that a peak current of 14 pA was elicited when the voltage was stepped from a holding potential of −70 to −20 mV. d_{Na} and f_{Na} represent the Hodgkin–Huxley type gating variables for activation and inactivation respectively. Their steady-state curves were taken from Holm *et al.*[19] The equation for the activation time constant was obtained by fitting data at −60 and 0 mV extrapolated from time-to-peak measurements. Similarly, the inactivation time constant was fitted to data at −50 and −10 mV. The R^2 value of both fits was 0.99. Model parameters were adjusted to 37 °C using a Q_{10} of 2.45, a value obtained by comparison of inactivation time constants at 10 °C and 21 °C measured in freshly dispersed cells from the rat gastric fundus.[36]

Non-Selective Cationic Channels

Non-selective cationic channels (NSCC) have been described in guinea-pig[26] and canine[45,54] gastric SM as well as in the guinea-pig ileum[23,24] and murine colon.[29]

$$I_{NSCC} = G_{NSCC} * m_{nscc} * r_{lig} * h_{Ca} * (V_m - E_{NSCC}) \quad (11)$$

G_{NSCC} represents the maximal conductance and its value (50 nS) was chosen yield an I–V profile that matches the one experimentally recorded in canine gastric SM cells under voltage clamp conditions where voltage was held at −60 mV and then brought from −120 mV to −10 mV with ramp commands.[45] m_{NSCC}represents the voltage dependency of the activation kinetics. Its steady state curve was also obtained from canine gastric data[45] however, in absence of a detailed kinetic description from canine gastric SM, the time constant was fitted to data from guine-pig ileum.[23] r_{lig} takes into account the observation that NSCC are activated experimentally by the presence of particular ligands (muscarinic stimulation). One such formulation can be obtained from isolated SM cells from the guinea-pig ileum.[23] The authors found that the effect of acetylcholine on the cellular response could be described with a Michaelis–Menten equation with a K_m value of 10 μM and a Hill coefficient of 1. The variable h_{Ca} was introduced in order to describe the facilitation effect that intracellular Ca^{2+} has on I_{NSCC} and was formulated as shown below.

$$h_{Ca} = \frac{1}{1 + \left(\frac{[Ca^{2+}]_i}{K_{CaNSCC}}\right)^{n_{Ca}}} \quad (12)$$

The values of the parameters K_{CaNSCC} (200 nM) and n_{Ca} (−4) were taken from the guinea-pig ileum[24] where values of 200 nM and 1 μM were obtained for half-maximal and sub-maximal Ca^{2+} concentrations respectively. The value of the reversal potential E_{NSCC} (−28 mV) was taken from canine pyloric SM data.[54]

Background Potassium Conductance

A background potassium conductance was included as described by

$$I_{Kb} = G_{Kb} * (V_m - E_K) \quad (13)$$

The value of the conductance G_{Kb} (0.0014 nS) was chosen in order to yield a stable resting membrane potential equal to that observed experimentally in canine gastric SM.[58]

Calcium Homeostasis

Control of the intracellular Ca^{2+} concentration is of primary importance as Ca^{2+} mediates a variety of processes including the regulation of several types of ion channels. The influx of Ca^{2+} from the extracellular space is mediated by plasma membrane Ca^{2+} channels. Ionic exchangers and intracellular stores such as the sarcoplasmic reticulum (SR) also play a significant role in maintaining intracellular Ca^{2+} homeostasis. The SR was found to be co-localized with Na^+/Ca^{2+} exchangers[35] and spatially closely associated with the plasma membrane.[41] In absence of contraction, Ca^{2+} influx through the L-type membrane channels does not appear to elicit a significant Ca^{2+} release from the SR during SMD.[7,27,60] The SR therefore adopts primarily a storage role (with Ryanodine and IP3-sensitive stores).[7,59] Moreover, it was observed that the rate of Ca^{2+} uptake is voltage independent[7] and that Na^+/Ca^{2+} exchanger activity did not contribute directly to the rate of decline of intracellular Ca^{2+}.[7] Plasma membrane Ca^{2+} pumps (PMCA)[22,34] and mitochondrial uptake[41] have also been indicated as homeostatic mechanisms for cytoplasmic Ca^{2+}.

Due to a lack of experimental data describing the mechanisms of intracellular Ca^{2+} control in gastric SM cells we have implemented a phenomenological model of Ca^{2+} uptake and extrusion. By grouping together the aforementioned components, we propose the following equation to describe the depletion of free Ca^{2+} ions from the intracellular space

$$I_{\mathrm{CaExt}} = 0.317 * [\mathrm{Ca}^{2+}]_i^{1.34} \tag{14}$$

I_{CaExt} (in mM/ms) therefore represents the total rate of Ca^{2+} uptake by the SR, mitochondria and extrusion via PMCA. The parameters in Eq. (14) were chosen to ensure Ca^{2+} homeostasis and that a physiological level of $[Ca]_i$ was achieved during each SMD.

Electrical Stimulus from ICC

The stimulus from the ICC network was modeled as an injected current whose value was obtained by dividing experimental (voltage) recordings of ICC from guinea pig gastric antrum by the value of the coupling resistance between ICC and SM. We chose an ICC profile with an amplitude of 59 mV[42] and a duration of just under 10 s.[11,15,18,43] The upstroke phase was characterized with a maximum gradient of 600 mV/s to reproduce experimental observations in canine gastric SM.[58]

The coupling between ICC and SM was studied by Cousins *et al.*[11] with experiments on guinea pig gastric antrum tissue samples. The value of the overall bulk coupling resistance between ICC and the nearby muscle layer (longitudinal and circular) was found to be 306 nS, representing the mean value of four measurements ranging from 157 to 877 nS. This value should be interpreted as a bulk tissue conductance and not the coupling conductance between a single ICC and a single SM cell. Indeed using this as a coupling conductance produced SM membrane potentials that were significantly higher than the normal physiological range. It was therefore necessary to adopt a much smaller value (1.3 nS) for the cell–cell coupling conductance to restrict the stimulus current to a more realistic amplitude. Figure 3 shows the ICC slow wave profile used to excite the SM cell model presented here.

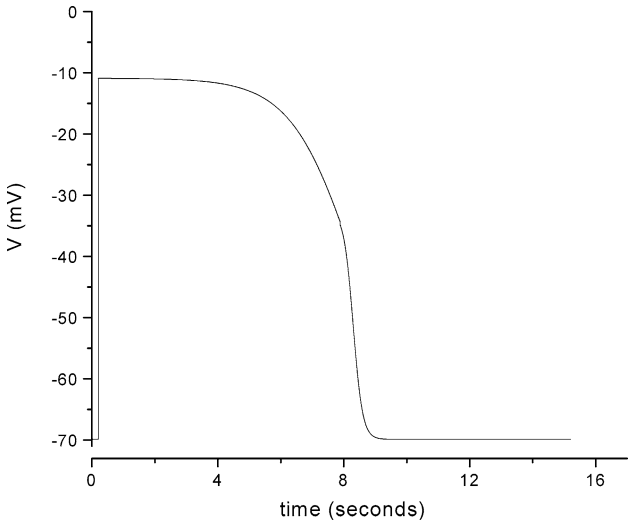

FIGURE 3. Slow wave profile of an ICC designed to reproduce experimental traces recorded from the guinea-pig gastric antrum. The voltage of this slow wave was divided by a coupling resistance and injected into the SM cell.

RESULTS

The results from a simulation showing a series of SMDs in the absence of muscarinic stimulation ([ACh] = 10 nM) are shown in Fig. 4. Experimentally recorded SMDs from a canine antral smooth muscle strip are also displayed.[58] The shape of the simulated SMD resembles those published in the literature[42,58] and the typical phases (upstroke, notch, plateau, and repolarization) can be clearly identified. The amplitude of the SMD was slightly more than 30 mV, consistent with experimental findings[20,21,43,49] and the membrane potential repolarization was 98% complete after 10 s in agreement with published experimental data.[21,43]

Figure 5 shows the time dependency of several of the main model variables. In experiments on canine gastric SM cells, SMDs caused an increase in intracellular Ca^{2+} concentration of approximately 200 nM.[55] Other reports on different SM found an increase on the order of 400 nM (reviewed in Carl *et al.*[9]). Our simulation results predict a rise in intracellular Ca^{2+}, as a result of Ca^{2+} influx through ion channels and intracellular uptake, of 300 nM in line with the experimental observations.

Potassium Channels Blockers

A-type potassium channels have been implicated in setting the membrane resting potential, however their contribution to the plateau phase of a SMD was found to be limited. In experiments with murine gastric SM cells the presence of flecainide (a known A-type channel blocker) in concentrations near its IC50 raised the resting membrane potential by 8.1%.[3] Here we simulated the presence of flecainide by halving the A-type potassium conductance. The results of this simulation (Fig. 6a) show a 5.7% rise in the resting membrane potential but no significant difference in the plateau potential.

The effect of another common potassium channel inhibitor 4-aminopyridine (4-AP) on the SMD was studied in feline gastric[6] canine colonic[51] and

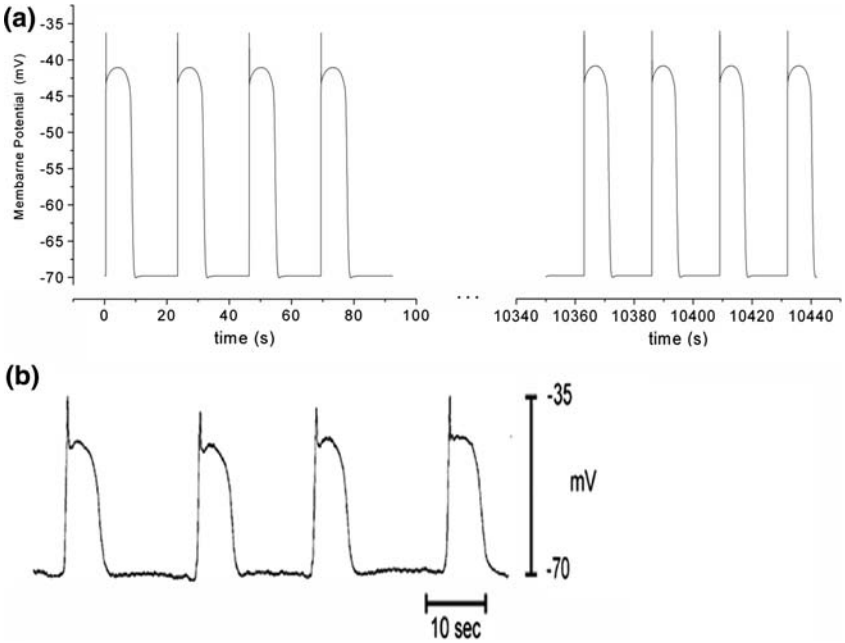

FIGURE 4. Simulation results: (a) modelled SMD at the beginning of the simulation and after 17 min of simulated activity at 2.6 cycles per minute (cpm); (b) Experimental recording obtained from canine gastric SM strip; reproduced from Ward *et al.*[58] with permission.

guinea-pig airway SM.[25] 4-AP in a concentration of 5 mM is a known blocker of both A-type and delayed rectifier potassium conductances (reviewed in Sanders *et al.*[42]) and therefore its presence was simulated by setting both the A-type and delayed rectifier conductances to zero. The simulated resting potential was raised by 10.5 mV (shown in Fig. 6b), in agreement with the 10–20 mV depolarization in the resting potential observed experimentally.[25] Moreover, the simulated plateau potential was raised by 5 mV which is consistent with the notion that the presence of 4-AP enhances contractility and the appearance of spike potentials observed in guinea-pig gastric antrum due to the increased level of the plateau potential.[6]

Experiments on intact SM preparations from canine colonic myocytes revealed that the addition of a potent BK channel blocker such as tetrapentylammonium (TPeA) extracellularly in concentrations of 20 μM (about 10 times its K_d value) caused a rise of 7 mV in the plateau phase of the SMD and eventually 'locked' the membrane potential at the plateau level as the repolarization failed to occur.[8] Here we simulated the presence of TPeA by shutting down the BK conductance ($G_{BK} = 0$). The result of this simulation (Fig. 6c) was a rise in the plateau by 4.6 mV. In our simulations, however, the membrane does not fail to repolarize as observed experimentally; a possible explanation for this discrepancy may be the effect of TPeA on the ICC in the intact muscle preparation as this is not incorporated here.

Effects of Intracellular Calcium on Calcium, and BK Channels

During a SMD the Ca^{2+} concentration in the cytoplasm rises as a result of the ionic influx through voltage gated Ca^{2+} channels. If the amount reaches a certain threshold spike potentials can be observed in the antral and pyloric regions and a contractile response occurs.[42] The regulatory mechanisms of the plateau phase of the SMDs have been attributed to the interplay between Ca^{2+} and potassium channels. The presence of Ca^{2+}-activated potassium channels in gastric muscle is expected to cause decreased plateau potentials in response to an increased (depolarizing) Ca^{2+} current through Ca^{2+} channels. Here the effects of an altered intracellular Ca^{2+} transient were simulated by modifying the inhibitory effect that Ca^{2+} ions have on L-type Ca^{2+} channels, i.e., releasing or tightening the self regulatory mechanism of L-type Ca^{2+} channels through the variable f_{Ca}. Partial inhibition of the regulatory mechanism was simulated by shifting the steady state curve of the variable f_{Ca} (half inactivation value shifted to 400 nM). By partially and completely inhibiting this negative feedback mechanism (see Fig. 7 for details), the plateau Ca^{2+} level was predicted to be 500 and 630 nM, respectively. This

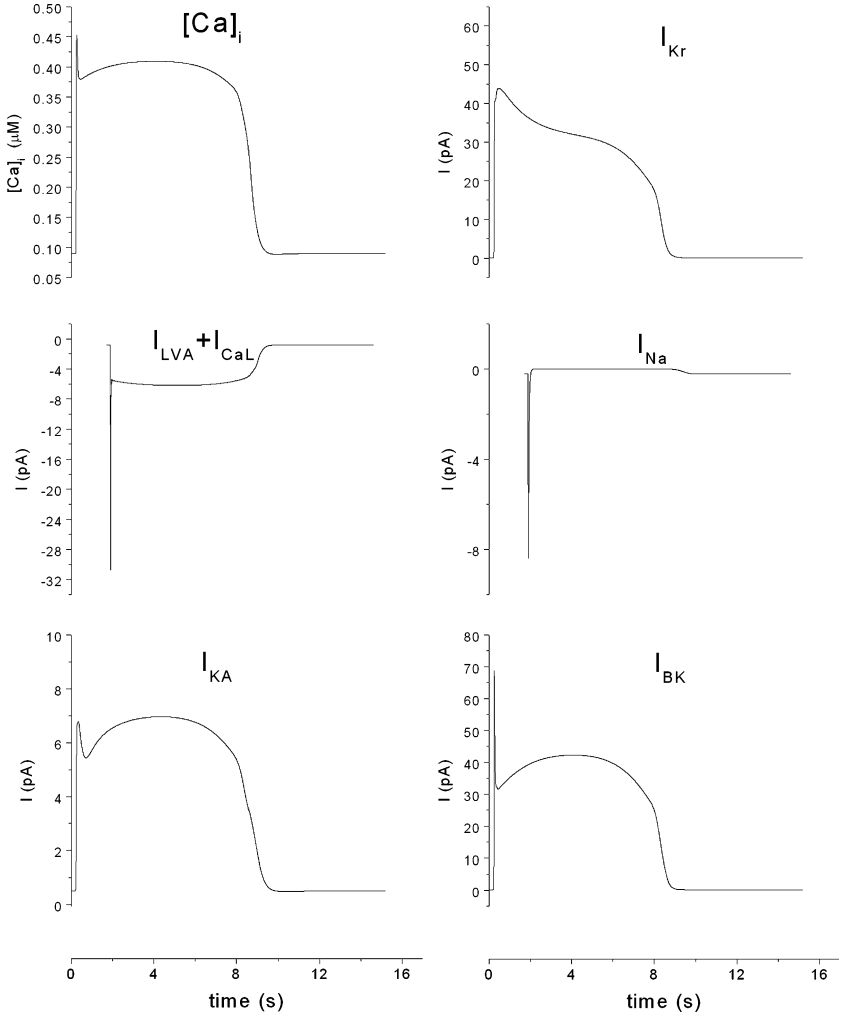

FIGURE 5. The main currents in the model are displayed over time for a single SMD along with the profile of the intracellular calcium transient (top left panel).

triggered an increased BK current (around 53 and 70 pA, respectively) which, despite an increase in the inward Ca^{2+} current, caused a shift in the plateau membrane potential in the polarized direction.

These results seem to support the view that during activation in phasic muscles, Ca^{2+}-activated BK channels may act as intracellular Ca^{2+} sensors and limit the degree of depolarization and contraction.[9]

DISCUSSION

The main objective of this work was to develop and validate a model of a gastric SM cellular electrophysiology. Due to the multitude of ion channel species present in such cells, the present description includes only those components that were deemed to significantly contribute to the cellular electrical response to a stimulation coming from the ICC network during basal electrical activity. For those ionic currents whose activation is mediated by the presence of, for example, particular ligands, we have chosen to either group the channel species into one component or to exclude them from the present description. The main reason for these simplifications is a lack of quantitative experimental data. These simplifications do, however, mean that only a relatively small number of equations are needed to describe the system making it suitable for large scale multi-cellular studies.

The trade-off between opposing needs of simplicity for computational efficiency and complexity for a complete description of the physiological reality resulted in a total of eight ionic currents, four of which are carried by potassium ions. The variety of potassium channels that has been identified so far in GI smooth muscle posed a challenge in determining which

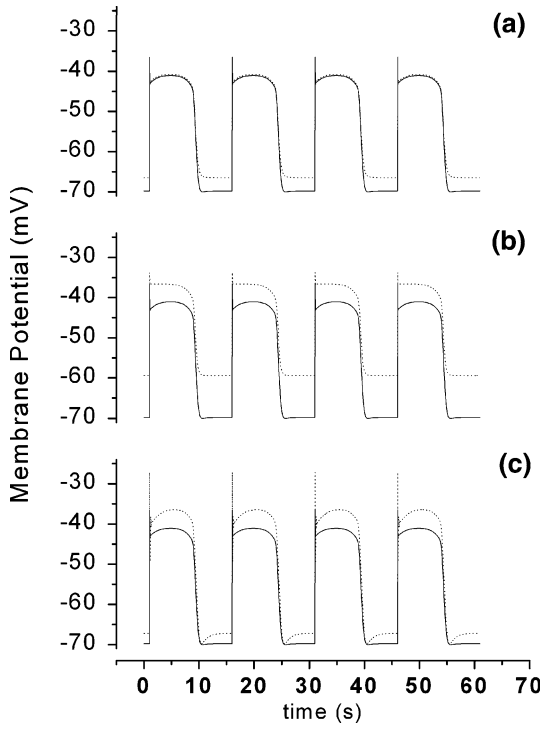

FIGURE 6. Effects of channel blockers on the SMD profile: (a) simulated presence of flecainide (30 μM) causing blockage of 50% of the A-type potassium conductance (dotted line) compared to control conditions (solid line); (b) simulated presence of 4-AP (5 mM) with blockage of A-type and delayed rectifier potassium currents (dotted line) compared to control conditions (solid line); (c) simulated presence of TPeA (20 μM) with blockage of BK channels (dotted line) compared to control conditions (solid line).

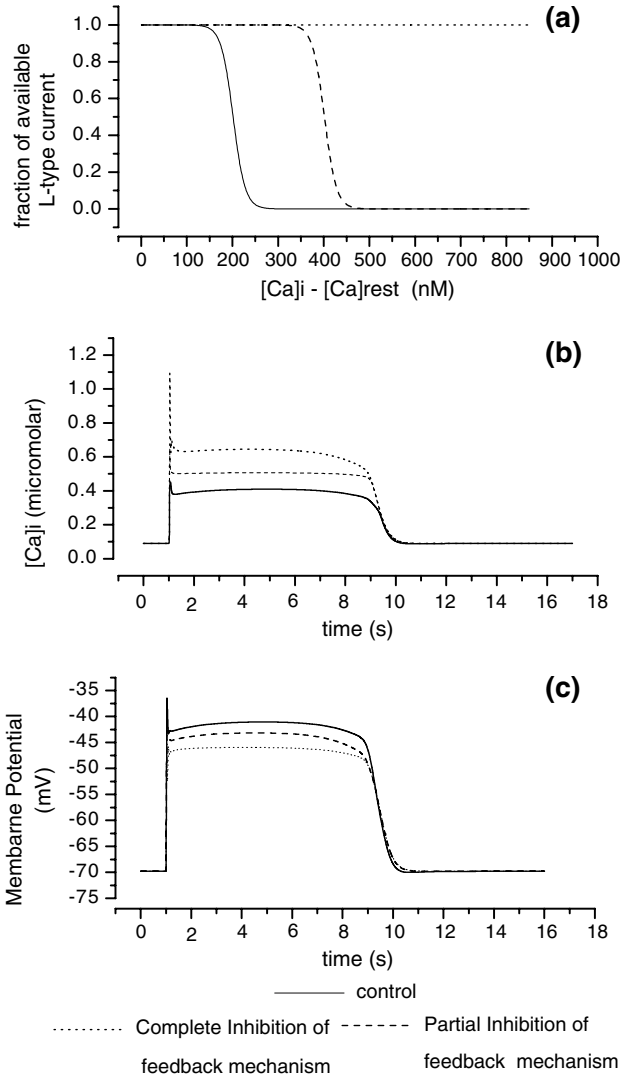

FIGURE 7. Comparison between the normal situation and the case of partial and complete inhibition of the $[Ca^{2+}]_i$ influence on L-type Ca^{2+} channels: (a) different curves used for the variable f_{Ca}. $h_{Ca} = 201.4$ nM for the control case, and 401.4 nM for the partially inhibited case. $s_{Ca} = 13.1$ in both cases. $f_{ca} = 1$ when the feedback is completely inhibited; (b) and (c) Influence of the feedback mechanism on cytoplasmic Ca^{2+} concentration and the SMD respectively.

ones to include as major players during the omnipresent electrical activity in the stomach. We grouped the so-called 'Two-Pore' K^+ (families of TREK and TASK channels) and the ether-a-go-go (ERG) channels in the background potassium current, that is believed to influence the resting membrane potential, without characterizing their response to particular stimuli. ATP-dependent potassium channels (K_{ATP}) were not included but would arguably be required to describe the response of a cell to metabolic stimuli (such as a drop in the ATP concentration below 1 mM) or ischemic conditions.[42]

The presence of chloride currents in gastrointestinal SM has not yet been fully demonstrated. Some pharmacological studies seem to imply the presence of such currents,[39,57] however the non-specificity of the drugs used in these studies together with the lack of a genotypic identification of such channels leaves the topic controversial. For this reason we decided not to include any Ca^{2+}-activated Chloride conductance. A volume-sensitive chloride conductance has also been reported in SM cells from guinea-pig stomach,[62] however, since in the present model we are not considering any mechanical deformations, this conductance has not been included.

Due to the fact that sodium and potassium ions generally do not possess the same ability to act as second messengers for important intracellular regulatory mechanisms as Ca^{2+} does, only the Ca^{2+} ion concentration was tracked whereas the K^+ and Na^+ concentrations were considered invariant. Quantitative data regarding the kinetics and regulatory aspects of intracellular Ca^{2+} ions dynamics are difficult to obtain and, as a consequence, the available literature is incomplete. Although it is known that intracellular Ca^{2+} uptake is dependent on the combined activity of

SR, mitochondria and PMCA, it is not known how the contribution of each uptake pathway affects the overall Ca^{2+} dynamics in the cytoplasm. Owing to these limitations, we summarized the intracellular Ca^{2+} uptake with one equation (Eq. 14) assuming that all intracellular uptake pathways depend only on the intracellular Ca^{2+} concentration itself. Such simplifications can be addressed in the future when sufficient experimental data becomes available.

Over the past few decades, patch clamp experiments have been performed on SM cells from different regions of the GI tract and from several different animal species. Inter-species differences in the electrophysiological properties of muscular tissues are widely reported. Moreover, within the same species, prominent regional differences between different tissues in the GI tract in terms of SMD shape, frequency and duration have been noted and attributed to different underlying cellular mechanisms. We found that there was not enough experimental data available to construct a complete model of a gastric SM cell from a single animal species. We have adopted experimental data from canine gastric SM cells whenever possible and when such data were not available, we preferentially included data from gastric SM cells from other species, and finally SM data from other GI regions.

While the resulting description is predominantly a description of a canine gastric SM cell, the limitations inherent in adopting data from other GI SM cells should not be ignored when interpreting model results, in particular where the goal is to relate an observed behavior to the underlying physiology. Nevertheless, the simulated SMD traces share many common features with those recorded experimentally from canine gastric SM preparations (Fig. 4). Simulated intracellular Ca^{2+} dynamics also resembled experimental measurements from canine gastric preparations. In order to further validate the model, we simulated the presence of known channel blockers or inhibitors by accordingly modifying the equation of that specific channel and checked whether the predicted SMD outcome matched the experimental SMD recording in presence of that specific blocker (Fig. 6). Results of such simulations are also in agreement with experimental data.

Although the results presented here are encouraging, much has to be done in order to establish electrophysiological models of the stomach as a reliable tool for investigating the pathophysiological aspects of this tissue in the same way as is done for the heart. The development of a complementary gastric ICC model and subsequent incorporation into multicellular tissue-level simulations will allow a better understanding of the mechanisms underlying electrophysiological abnormalities as are seen in gastric arrhythmias, gastroparesis, and other gastric disorders.

APPENDIX

The main equations of the model are:

$$C_m \frac{dV_m}{dt} = -(I_{ion} + I_{stim})$$

$$I_{ion} = I_{CaL} + I_{LVA} + I_{Kr} + I_{Ka} + I_{BK} + I_{Kb} + I_{Na} + I_{NSCC}$$

$$I_{stim} = \begin{cases} G_{couple} * \Delta V_{ICC} & t < t_{ICCpeak} \\ G_{couple} * \Delta V_{ICC} * \frac{1}{1+e^{\frac{t-8000}{1000}}} & t_{ICCpeak} < t < t_{ICCplateau} \\ I_{stim}(t=t_{ICCplateau}) * \frac{1.3}{1+e^{\frac{t-8000}{150}}} & t_{ICCplateau} < t < t_{ICC} \end{cases}$$

$$\frac{d[Ca]_i}{dt} = -\frac{I_{caL} + I_{caT}}{2 * F * V_c} - I_{CaExt}$$

- *Steady state parameters*

Activation: $\frac{1}{1+e^{-\frac{V_{0.5}+V}{k}}}$ Inactivation: $\frac{1}{1+e^{\frac{V_{0.5}+V}{k}}}$

Activation			Inactivation		
Variable name	$V_{0.5}$ (mV)	k	Variable name	$V_{0.5}$ (mV)	k
d	17	4.3	f	43	8.9
d_{LVA}	27.5	10.9	f_{LVA}	15.8	7
x_{r1}	27	5	x_{r2}*	58	10
x_{a1}	26.5	7.9	x_{a2}**	65	6.2
d_{Na}	47	4.8	f_{Na}	78	3
m_{NSCC}	25	20			

* For this variable the equation was used in the form: $\frac{0.8}{1+e^{\frac{V_{0.5}+V}{k}}} + 0.2$.

** For this variable the equation was used in the form: $\frac{0.9}{1+e^{\frac{V_{0.5}+V}{k}}} + 0.1$.

- *Time constants*

Variable name	Time constants (ms)
d	0.47
f	86
d_{LVA}	3
f_{LVA}	$7.58 * e^{0.00817 * V_m}$
x_{r1}	80
x_{r2}	$-707.0 + 1481 * e^{\frac{V_m+36}{95}}$
x_{a1}	$31.8 + 175 * e^{-0.5*(\frac{V_m+44.4}{22.3})^2}$
x_{a2}	90
d_{Na}	$-0.017^* V_m + 0.44$
f_{Na}	$-0.25^* V_m + 5.5$
m_{NSCC}	$\frac{150}{1+e^{\frac{V_m+66}{26}}}$

Model parameters

Parameter name	Description	Value	Units
R	Ideal gas constant	8.314	J/(mol*K)
T	Temperature	310	K

Parameter name	Description	Value	Units
F	Faraday constant	96486.7	C/mol
C_m	Cell membrane capacitance	77	pF
A_m	Cell surface	0.000041	cm^2
V_c	Total cytoplasmic volume	3500	μm^3
Ca_o	Extracellular Ca^{2+} concentration	2.5	mM
Na_o	Extracellular sodium concentration	137	mM
Na_i	Intracellular sodium concentration	10	mM
K_o	Extracellular potassium concentration	5.9	mM
K_i	Intracellular potassium concentration	164	mM
Ach	Acetylcholine concentration in absence of muscarinic stimulation	10	nM
G_{CaL}	Maximal conductance for L-type Ca^{2+} channels	65	nS
G_{LVA}	Maximal conductance for low-voltage activated Ca^{2+} channels	0.18	nS
G_{Kr}	Maximal conductance for delayed rectifier potassium channels	35	nS
G_{Ka}	Maximal conductance for A-type potassium channels	9	nS
G_{BK}	Maximal conductance for Ca^{2+}-activated potassium channels	45.7	nS
G_{Kb}	Maximal background potassium conductance	0.014	nS
G_{Na}	Maximal conductance for sodium channels	3	nS
G_{NSCC}	Maximal conductance for non-selective cationic channels	50	nS
G_{couple}	Coupling conductance between ICC and SM	1.3	nS
h	Steepness for Ca^{2+} activation for BK channels	2	–
K_{bk}	Steepness for voltage activation for BK channels	−17	mV
Ca_{set}	Ca^{2+} set point for BK channels	0.001	mM
h_{Ca}	Half concentration for the f_{Ca} variable	201.4	nM
s_{Ca}	Slope factor for the steady state f_{Ca} variable	13.1	nM
E_{NSCC}	Reversal potential for NSCC channels	−28	mV
$K_{m\text{-}NSCC}$	Half activation value for Ach activation of NSCC channels	10	μM
n_{Ach}	Hill coefficient for Ach activation of NSCC channels	1	–
$K_{Ca\text{-}NSCC}$	Half activation value for Ca^{2+} facilitation of NSCC channels	200	nM
n_{Ca}	Hill coefficient for Ca^{2+} facilitation of NSCC channels	−4	–
$Q_{10\text{-}Ca}$	Q_{10} value for Ca^{2+} channels	2.1	–
$Q_{10\text{-}K}$	Q_{10} value for potassium channels	1.5	–
$Q_{10\text{-}Na}$	Q_{10} value for sodium channels	2.45	–
ΔV_{ICC}	Membrane potential fluctuation in an ICC	59	mV
$t_{ICCpeak}$	Peak time of the slow wave in an ICC	98	ms
$t_{ICCplateau}$	Plateau time of the slow wave in the ICC	7582	ms
t_{ICC}	Total time of the slow wave in the ICC	10,000	ms

ACKNOWLEDGMENTS

The authors are grateful to Dr. K. Sanders and Dr. G. Farrugia for their advice.

SUPPLEMENTAL MATERIAL

A sample implementation of the model is available from the authors upon request.

REFERENCES

[1]Akbarali, H. I., and W. R. Giles. Ca2+ and Ca(2+)-activated Cl^- currents in rabbit oesophageal smooth muscle. *J. Physiol.* 460:117–133, 1993.

[2]Aliev, R. R., W. Richards, and J. P. Wikswo. A simple nonlinear model of electrical activity in the intestine. *J. Theor. Biol.* 204:21–28, 2000.

[3]Amberg, G. C., S. A. Baker, S. D. Koh, W. J. Hatton, K. J. Murray, B. Horowitz, and K. M. Sanders. Characterization of the A-type potassium current in murine gastric antrum. *J. Physiol.* 544:417–428, 2002.

[4]Amberg, G. C., S. D. Koh, Y. Imaizumi, S. Ohya, and K. M. Sanders. A-type potassium currents in smooth muscle. *Am. J. Physiol. Cell. Physiol.* 284:C583–C595, 2003.

[5]Barrett, J. N., K. L. Magleby, and B. S. Pallotta. Properties of single calcium-activated potassium channels in cultured rat muscle. *J. Physiol.* 331:211–230, 1982.

[6]Boev, K., A. Bonev, and M. Papasova. 4-Aminopyridine-induced changes in the electrical and contractile activities of the gastric smooth muscle. *Gen. Physiol. Biophys.* 4:589–595, 1985.

[7]Bradley, K. N., E. R. Flynn, T. C. Muir, and J. G. McCarron. Ca(2+) regulation in guinea-pig colonic smooth muscle: the role of the Na(+)–Ca(2+) exchanger and the sarcoplasmic reticulum. *J. Physiol.* 538:465–482, 2002.

[8]Carl, A., B. W. Frey, S. M. Ward, K. M. Sanders, and J. L. Kenyon. Inhibition of slow-wave repolarization and

Ca(2+)-activated K+ channels by quaternary ammonium ions. *Am. J. Physiol.* 264:C625–C631, 1993.
[9]Carl, A., H. K. Lee, and K. M. Sanders. Regulation of ion channels in smooth muscles by calcium. *Am. J. Physiol.* 271:C9–C34, 1996.
[10]Casteels, R. Membrane potential in smooth muscle. In: Smooth Muscle: An Assesment of Current Knowledge, edited by E. B. A. Bulbring, A. W. Jones and T. Tomita. London: Edward Arnold, 1981, pp. 105–126.
[11]Cousins, H. M., F. R. Edwards, H. Hickey, C. E. Hill, and G. D. Hirst. Electrical coupling between the myenteric interstitial cells of Cajal and adjacent muscle layers in the guinea-pig gastric antrum. *J. Physiol.* 550:829–844, 2003.
[12]Edwards, F. R., and G. D. Hirst. An electrical description of the generation of slow waves in the antrum of the guinea-pig. *J. Physiol.* 564:213–232, 2005.
[13]Farrugia, G. Ionic conductances in gastrointestinal smooth muscles and interstitial cells of Cajal. *Annu. Rev. Physiol.* 61:45–84, 1999.
[14]Farrugia, G., A. Rich, J. L. Rae, M. G. Sarr, and J. H. Szurszewski. Calcium currents in human and canine jejunal circular smooth muscle cells. *Gastroenterology* 109:707–717, 1995.
[15]Forrest, A. S., T. Ordog, and K. M. Sanders. Neural regulation of slow wave frequency in the murine gastric antrum. *Am. J. Physiol. Gastrointest. Liver Physiol.* 290(3):G486–G495, 2005.
[16]Ganitkevich, V., M. F. Shuba, and S. V. Smirnov. Calcium-dependent inactivation of potential-dependent calcium inward current in an isolated guinea-pig smooth muscle cell. *J. Physiol.* 392:431–449, 1987.
[17]Hagiwara, S., K. Kusano, and N. Saito. Membrane changes of Onchidium nerve cell in potassium-rich media. *J. Physiol.* 155:470–489, 1961.
[18]Hirst, G. D., and F. R. Edwards. Role of interstitial cells of Cajal in the control of gastric motility. *J. Pharmacol. Sci.* 96:1–10, 2004.
[19]Holm, A. N., A. Rich, S. M. Miller, P. Strege, Y. Ou, S. Gibbons, M. G. Sarr, J. H. Szurszewski, J. L. Rae, and G. Farrugia. Sodium current in human jejunal circular smooth muscle cells. *Gastroenterology* 122:178–187, 2002.
[20]Huang, S., S. Nakayama, S. Iino, and T. Tomita. Voltage sensitivity of slow wave frequency in isolated circular muscle strips from guinea pig gastric antrum. *Am. J. Physiol.* 276:G518–G528, 1999.
[21]Huizinga, J. D. Physiology and pathophysiology of the interstitial cell of Cajal: from bench to bedside. II. Gastric motility: lessons from mutant mice on slow waves and innervation. *Am. J. Physiol. Gastrointest. Liver Physiol.* 281:G1129–G1134, 2001.
[22]Hurwitz, L., D. F. Fitzpatrick, G. Debbas, and E. J. Landon. Localization of calcium pump activity in smooth muscle. *Science* 179:384–386, 1973.
[23]Inoue, R., and G. Isenberg. Effect of membrane potential on acetylcholine-induced inward current in guinea-pig ileum. *J. Physiol.* 424:57–71, 1990.
[24]Inoue, R., and G. Isenberg. Intracellular calcium ions modulate acetylcholine-induced inward current in guinea-pig ileum. *J. Physiol.* 424:73–92, 1990.
[25]Isaac, L., S. McArdle, N. M. Miller, R. W. Foster, and R. C. Small. Effects of some K(+)-channel inhibitors on the electrical behaviour of guinea-pig isolated trachealis and on its responses to spasmogenic drugs. *Br. J. Pharmacol.* 117:1653–1662, 1996.
[26]Kang, T. M., Y. C. Kim, J. H. Sim, J. C. Rhee, S. J. Kim, D. Y. Uhm, I. So, and K. W. Kim. The properties of carbachol-activated nonselective cation channels at the single channel level in guinea pig gastric myocytes. *Jpn. J. Pharmacol.* 85:291–298, 2001.
[27]Kim, S. J., S. C. Ahn, J. K. Kim, Y. C. Kim, I. So, and K. W. Kim. Changes in intracellular Ca2+ concentration induced by L-type Ca2+ channel current in guinea pig gastric myocytes. *Am. J. Physiol.* 273:C1947–C1956, 1997.
[28]Knot, H., J. Brayden, and M. Nelson. Calcium channels and potassium channels. In: Biochemistry of Smooth Muscle Contraction., edited by M. Barany. Chicago: Academic Press, 1995, pp. 203–217.
[29]Koh, S. D., K. Monaghan, S. Ro, H. S. Mason, J. L. Kenyon, and K. M. Sanders. Novel voltage-dependent non-selective cation conductance in murine colonic myocytes. *J. Physiol.* 533:341–355, 2001.
[30]Koh, S. D., S. M. Ward, G. M. Dick, A. Epperson, H. P. Bonner, K. M. Sanders, B. Horowitz, and J. L. Kenyon. Contribution of delayed rectifier potassium currents to the electrical activity of murine colonic smooth muscle. *J. Physiol.* 515(Pt 2):475–487, 1999.
[31]Lang, R. J., and C. A. Rattray-Wood. A simple mathematical model of the spontaneous electrical activity in a single smooth muscle myocyte. In: Smooth Muscle Excitation, edited by B. Bolton and T. Tomita. London: Academic Press, 1996, pp. 391–402.
[32]Langton, P. D., E. P. Burke, and K. M. Sanders. Participation of Ca currents in colonic electrical activity. *Am. J. Physiol.* 257:C451–C460, 1989.
[33]Miftakhov, R. N., G. R. Abdusheva, and J. Christensen. Numerical simulation of motility patterns of the small bowel. 1. formulation of a mathematical model. *J. Theor. Biol.* 197:89–112, 1999.
[34]Monteith, G. R., E. P. Kable, S. Chen, and B. D. Roufogalis. Plasma membrane calcium pump-mediated calcium efflux and bulk cytosolic free calcium in cultured aortic smooth muscle cells from spontaneously hypertensive and Wistar-Kyoto normotensives rats. *J. Hypertens* 14:435–442, 1996.
[35]Moore, E. D., E. F. Etter, K. D. Philipson, W. A. Carrington, K. E. Fogarty, L. M. Lifshitz, and F. S. Fay. Coupling of the Na+/Ca2+ exchanger, Na+/K+ pump and sarcoplasmic reticulum in smooth muscle. *Nature* 365:657–660, 1993.
[36]Muraki, K., Y. Imaizumi, and M. Watanabe. Sodium currents in smooth muscle cells freshly isolated from stomach fundus of the rat and ureter of the guinea-pig. *J. Physiol.* 442:351–375, 1991.
[37]Noack, T., P. Deitmer, and E. Lammel. Characterization of membrane currents in single smooth muscle cells from the guinea-pig gastric antrum. *J. Physiol.* 451:387–417, 1992.
[38]Noble, D. Modeling the heart. *Physiology (Bethesda)* 19:191–197, 2004.
[39]Ohta, T., S. Ito, and Y. Nakazato. Chloride currents activated by caffeine in rat intestinal smooth muscle cells. *J. Physiol.* 465:149–162, 1993.
[40]Pullan, A., L. Cheng, R. Yassi, and M. Buist. Modelling gastrointestinal bioelectric activity. *Prog. Biophys. Mol. Biol.* 85:523–550, 2004.
[41]Sanders, K.M. Invited review: mechanisms of calcium handling in smooth muscles. *J. Appl. Physiol.* 91:1438–1449, 2001.
[42]Sanders, K., S. Koh, and S. Ward. Organization and electrophysiology of interstitial cells of cajal and smooth

muscle cells in the gastrointestinal tract. In: Physiology of the gastrointestinal tract, edited by L.R. Johnson. Boston: Elsevier Academic Press, 2006, pp. 533–576.
[43]Sanders, K. M., S. D. Koh, and S. M. Ward. Interstitial cells of cajal as pacemakers in the gastrointestinal tract. *Annu. Rev. Physiol.* 68:307–343, 2006.
[44]Sims, S. M. Calcium and potassium currents in canine gastric smooth muscle cells. *Am. J. Physiol.* 262:G859–G867, 1992.
[45]Sims, S. M. Cholinergic activation of a non-selective cation current in canine gastric smooth muscle is associated with contraction. *J. Physiol.* 449:377–398, 1992.
[46]Skinner, F. K., C. A. Ward, and B. L. Bardakjian. Pump and exchanger mechanisms in a model of smooth muscle. *Biophys. Chem.* 45:253–272, 1993.
[47]Smirnov, S. V., A. V. Zholos, and M. F. Shuba. A potential-dependent fast outward current in single smooth muscle cells isolated from the newborn rat ileum. *J. Physiol.* 454:573–589, 1992.
[48]Splawski, I., K. W. Timothy, L. M. Sharpe, N. Decher, P. Kumar, R. Bloise, C. Napolitano, P. J. Schwartz, R. M. Joseph, K. Condouris, H. Tager-Flusberg, S. G. Priori, M. C. Sanguinetti, and M. T. Keating. Ca(V)1.2 calcium channel dysfunction causes a multisystem disorder including arrhythmia and autism. *Cell* 119:19–31, 2004.
[49]Suzuki, H. Cellular mechanisms of myogenic activity in gastric smooth muscle. *Jpn. J. Physiol.* 50:289–301, 2000.
[50]ten Tusscher, K. H., D. Noble, P. J. Noble, and A. V. Panfilov. A model for human ventricular tissue. *Am. J. Physiol. Heart. Circ. Physiol.* 286:H1573–H1589, 2004.
[51]Thornbury, K. D., S. M. Ward, and K. M. Sanders. Participation of fast-activating, voltage-dependent K currents in electrical slow waves of colonic circular muscle. *Am. J. Physiol.* 263:C226–C236, 1992.
[52]Tiwari, J. K., and S. K. Sikdar. Temperature-dependent conformational changes in a voltage-gated potassium channel. *Eur. Biophys. J.* 28:338–345, 1999.
[53]Vivaudou, M. B., L. H. Clapp, J. V. Walsh Jr, and J. J. Singer. Regulation of one type of Ca2+ current in smooth muscle cells by diacylglycerol and acetylcholine. *Faseb. J.* 2:2497–2504, 1988.
[54]Vogalis, F., and K.M. Sanders. Cholinergic stimulation activates a non-selective cation current in canine pyloric circular muscle cells. *J. Physiol.* 429:223–236, 1990.
[55]Vogalis, F., N.G. Publicover, J.R. Hume, and K.M. Sanders. Relationship between calcium current and cytosolic calcium in canine gastric smooth muscle cells. *Am. J. Physiol.* 260:C1012–C1018, 1991.
[56]Vogalis, F., N. G. Publicover, and K. M. Sanders. Regulation of calcium current by voltage and cytoplasmic calcium in canine gastric smooth muscle. *Am. J. Physiol.* 262:C691–C700, 1992.
[57]Wang, Q., H. I. Akbarali, N. Hatakeyama, and R. K. Goyal. Caffeine- and carbachol-induced Cl- and cation currents in single opossum esophageal circular muscle cells. *Am. J. Physiol.* 271:C1725–C1734, 1996.
[58]Ward, S. M., R. E. Dixon, A. de Faoite, and K. M. Sanders. Voltage-dependent calcium entry underlies propagation of slow waves in canine gastric antrum. *J. Physiol.* 561:793–810, 2004.
[59]White, C., and J. G. McGeown. Regulation of basal intracellular calcium concentration by the sarcoplasmic reticulum in myocytes from the rat gastric antrum. *J. Physiol.* 529(Pt 2):395–404, 2000.
[60]Wu, C., and C. H. Fry. Na(+)/Ca(2+) exchange and its role in intracellular Ca(2+) regulation in guinea pig detrusor smooth muscle. *Am. J. Physiol. Cell. Physiol.* 280:C1090–C1096, 2001.
[61]Xiong, Z., N. Sperelakis, A. Noffsinger, and C. Fenoglio-Preiser. Ca2+ currents in human colonic smooth muscle cells. *Am. J. Physiol.* 269:G378–G385, 1995.
[62]Xu, W. X., S. J. Kim, I. So, T. M. Kang, J. C. Rhee, and K. W. Kim. Volume-sensitive chloride current activated by hyposmotic swelling in antral gastric myocytes of the guinea-pig. *Pflugers Arch.* 435:9–19, 1997.
[63]Yamamoto, Y., S. L. Hu, and C. Y. Kao. Inward current in single smooth muscle cells of the guinea pig taenia coli. *J. Gen. Physiol.* 93:521–550, 1989.
[64]Yoshino, M., T. Someya, A. Nishio, and H. Yabu. Whole-cell and unitary Ca channel currents in mammalian intestinal smooth muscle cells: evidence for the existence of two types of Ca channels. *Pflugers Arch.* 411:229–231, 1988.
[65]Yunker, A. M., and M. W. McEnery. Low-voltage-activated ("T-Type") calcium channels in review. *J. Bioenerg. Biomembr.* 35:533–575, 2003.